Kinetics and mechanism of the reaction of hydroxyl with benzene over 790–1410 K

ARTICLE *in* THE JOURNAL OF PHYSICAL CHEMISTRY · APRIL 1985

Impact Factor: 2.78 · DOI: 10.1021/j100262a026

2 AUTHORS, INCLUDING:

Sasha Madronich
National Center for Atmospheric Research
278 PUBLICATIONS **10,309** CITATIONS

Reprinted from The Journal of Physical Chemistry, 1985, 89, 3556.

Kinetics and Mechanism of the Reaction of OH with C_6H_6 over 790–1410 K

S. Madronich† and W. Felder*

AeroChem Research Laboratories, Inc., P.O. Box 12, Princeton, New Jersey 08542
(Received: December 10, 1984)

The AeroChem high temperature photochemistry (HTP) technique was used to study the reaction OH + C_6H_6 → products (1). Direct measurements of the overall rate coefficient $k_1(T)$ for this reaction were obtained over the temperature range 790–1410 K. The upper temperature of this work exceeds, by some 400 K, the upper temperature of any 100)/T] reported kinetic study on this reaction. The data are fitted by the expression $k_1(T) = (3.5 \pm 0.3) \times 10^{-11} \exp[-(2300 \pm 100)/T]$ cm^3 s^{-1}. Mechanistic studies near 1300 K showed that reaction 1 is dominated by the abstraction channel, OH + C_6H_6 → C_6H_5 + H_2O (1a). The effect of the reverse reaction, C_6H_5 + H_2O → OH + C_6H_6 (−1a), was also observed at suitably chosen experimental conditions, and its rate coefficient, k_{-1a}, was measured. The value of k_{-1a}, $(1.0 \pm 0.3) \times 10^{-14}$ cm^3 s^{-1}, was found to agree with estimates obtained from the measured forward rate coefficient, k_{1a}, and available thermochemical data. The 1300 K work also showed that a nonabstraction channel recently proposed by other workers on the basis of theoretical calculations, OH + C_6H_6 → C_6H_5OH + H (1b), does not contribute significantly (<20%) to the overall reaction rate.

I. Introduction

The formation and destruction of aromatic hydrocarbons in fuel-rich combustion is an area of intense study and interest because of the possible importance of such processes to mechanisms of soot generation (e.g., ref 1 and 2), to the combustion of aromatics, and to the formation and destruction of pollutant aromatics. The identity of the important elementary chemical steps and the values of their rate coefficients are among the major unknowns confronting modelers. It is, however, clear that the reactions of aromatic hydrocarbons with the ubiquitous flame radical OH play a major role in these processes.

The high-temperature oxidation of benzene (C_6H_6) has received considerable attention in recent years,[3-6] but no directly measured kinetic or mechanistic data have been available on the reaction

$$OH + C_6H_6 \rightarrow \text{products} \qquad (1)$$

at temperatures relevant to combustion ($T > 1000$ K).

Reaction 1 has been studied extensively at temperatures below about 600 K,[7-13] but only one direct study has so far been published[10] for higher temperatures (up to about 1020 K). At the lower temperatures, electrophilic addition is generally recognized as the most important reaction channel. Above 600 K, the single flash photolysis/resonance fluorescence study by Tully et al.[10] yielded an overall rate coefficient for the disappearance of OH of $k_1(T) = (2.4 \pm 0.9) \times 10^{-11} \exp[-(2260 \pm 300)/T]$ cm^3 molecule^{-1} s^{-1}. Isotopic substitution studies by these workers indicated that the reaction proceeds mainly via abstraction

$$OH + C_6H_6 \rightarrow C_6H_5 + H_2O \qquad (1a)$$

The existence of a second, high-temperature, nonabstraction channel for the reaction OH + C_6H_6 has been suggested by Bittner et al.,[4] based on benzene oxidation studies in low-pressure flames using molecular beam sampling mass spectrometry. Their measurements are consistent with a mechanism in which OH + C_6H_6 is the primary reaction for benzene consumption, but the observed low phenyl radical mole fractions imply that abstraction is a relatively minor channel of the OH + C_6H_6 reaction, with phenol and H being the favored products.

Venkat et al.[5] also observed large concentrations of phenol in turbulent flow reactor oxidation of benzene at ca. 1200 K, but attributed its formation to quenching of phenoxy radicals (produced by oxidation of the phenyl radical) in the sampling probe. However, Lin and co-workers[14,15] have proposed, on the basis of theoretical calculations, that above ca. 600 K the reaction OH + C_6H_6 proceeds exclusively by the mechanism

$$OH + C_6H_6 \rightleftarrows C_6H_6OH^{\ddagger} \rightarrow C_6H_5OH + H \qquad (1b)$$

for which the calculated rate coefficient is in excellent agreement with the measured rate coefficients of Tully et al.;[10] the abstraction channel was calculated to have a negligible contribution at all temperatures.

The high temperature photochemistry (HTP) technique used in the present study permits the use of a direct kinetic technique (flash photolysis/resonance fluorescence) at temperatures significantly higher than those achievable by conventional kinetic methods. We report here direct measurements of the overall rate coefficient for the OH + C_6H_6 reaction over the temperature range 790–1410 K and the results of detailed mechanistic studies performed near 1300 K. This study shows that near 1300 K the reaction mechanism is dominated by the abstraction channel.

II. Experimental Section

The high temperature photochemistry (HTP) technique used in this study is an extension to wider temperature ranges of the conventional flash photolysis/resonance fluorescence method. The HTP technique has been extensively validated in previous studies.[16-19]

The construction details of the HTP reactor have been described elsewhere.[19] Briefly, it consists of an alumina reaction tube, suitably heated and insulated. Reaction zone temperature,

† Present address: National Center for Atmospheric Research, P.O. Box 3000, Boulder, CO 80307.

(1) Frenklach, M.; Clary, D. W.; Gardiner, W. C., Jr.; Stein, S. E. *Symp. (Int.) Combust., [Proc.], 20th*, in press.
(2) Bockhorn, H.; Fetting, F.; Wenz, H. W. *Ber. Bunsenges. Phys. Chem.* **1983**, *87*, 1067.
(3) Bittner, J. D.; Howard, J. B. *Symp. (Int.) Combust., [Proc.], 18th* **1981**, 1105.
(4) Bittner, J. D.; Palmer, H. B.; Howard, J. B. In "Soot Formation in Combustion Systems and Its Toxic Properties", Lahaye, J., Prado, G., Eds.; Plenum: New York, 1983; p 95.
(5) Venkat, C.; Brezinsky, K.; Glassman, I. *Symp. (Int.) Combust., [Proc.], 19th* **1982**, 143.
(6) Fujii, N.; Asaba, T. *J. Fac. Eng., Univ. Tokyo* **1977**, *34*, 189.
(7) Davis, D. D.; Bollinger, W.; Fischer, S. *J. Phys. Chem.* **1975**, *79*, 293.
(8) Hansen, D. A.; Atkinson, R.; Pitts, J. N., Jr. *J. Phys. Chem.* **1975**, *79*, 1763.
(9) Perry, R. A.; Atkinson, R.; Pitts, J. N., Jr. *J. Phys. Chem.* **1977**, *81*, 296.
(10) Tully, F. P.; Ravishankara, A. R.; Thompson, R. L.; Nicovich, J. M.; Shah, R. C.; Kreutter, N. M.; Wine, P. H. *J. Phys. Chem.* **1981**, *85*, 2262.
(11) Wahner, A.; Zetzsch, C. *J. Phys. Chem.* **1983**, *87*, 4945.
(12) Lorenz, K.; Zellner, R. *Ber. Bunsenges. Phys. Chem.* **1983**, *87*, 629.
(13) Rinke, M.; Zetzsch, C. *Ber. Bunsenges. Phys. Chem.* **1984**, *88*, 55.
(14) Hsu, D. S. Y.; Lin, C. Y.; Lin, M. C. *Symp. (Int.) Combust., [Proc.], 20th*, in press.
(15) Lin, C. Y.; Lin, M. C. Presented at Fall Technical Meeting, Eastern States: The Combustion Institute, Clearwater, FL. December 3–5, 1984.
(16) Felder, W.; Fontijn, A. *Chem. Phys. Lett.* **1979**, *67*, 53.
(17) Madronich, S.; Felder, W. *J. Phys. Chem.* **1984**, *88*, 1857.
(18) Madronich, S.; Felder, W. *Symp. (Int.) Combust., [Proc.], 20th*, in press.
(19) Felder, W.; Fontijn, A.; Volltrauer, H. N.; Voorhees, D. R. *Rev. Sci. Instrum.* **1980**, *51*, 195.

0022-3654/85/2089-3556$01.50/0

TABLE I: OH + C_6H_6 Rate Coefficient Measurements

T, K	$\pm\sigma_T$, K	P, kPa	v, cm s^{-1}	$[H_2O]$, 10^{15} cm^{-3}	$[C_6H_6]$, 10^{13} cm^{-3}	flash window	flash energy, J	uncorrected k_1, 10^{-12} cm^3 s^{-1}	uncorrected $\pm\sigma_k$, 10^{-12} cm^3 s^{-1}	corrected k_1, 10^{-12} cm^3 s^{-1}	corrected $\pm\sigma_k$, 10^{-12} cm^3 s^{-1}
787	10	18.4	23	8.50	7.3–20.9	LiF	32	2.09	0.06	*a*	
805	10	18.6	23	1.38–2.88	5.2–34.0	LiF	72	1.78	0.06	*a*	
865	14	15.4	19–51	0.31–5.69	3.4–33.4	SiO_2	30	2.67	0.18	*a*	
1019	12	14.3	26	0.89–10.1	6.0–27.8	SiO_2	30	2.69	0.30	3.04	0.29
1196	16	17.4	34	1.17–4.22	2.1–15.7	SiO_2	30–85	2.88	0.20	3.52	0.25
1309	17	11.5	138	1.37	1.4–5.3	LiF	72	5.74	0.34	6.66	0.23
1314	17	11.7	137	5.36–6.00	3.2–15.4	LiF	72	*b*		*b*	
1409	21	11.6	150	1.18	1.3–5.3	LiF	72	5.72	0.93	7.36	1.12

*Not required. *b* $[H_2O]$ deliberately high for mechanistic studies. Not suitable for most accurate determination of k_1, but see entry at T = 1309 K.

pressure, and concentrations of reagents can be varied independently. Metered flows of gases are premixed and then admitted near the base of the reactor.

All experiments reported here were performed in Ar diluent (boil-off from the liquid). The H_2O vapor was produced by bubbling Ar through distilled H_2O at ambient pressure and temperature.

Samples of the C_6H_6 used in this work (Fisher, ACS certified, 99 mol %) were analyzed (Princeton Testing Laboratory) by GC/MS and were found to contain 41 mg L^{-1} (ca. 40 ppm) toluene, with no evidence of high boiling compounds. This low toluene concentration does not affect the kinetic measurements at any experimental condition. Before use, the C_6H_6 was outgassed by repeated freeze–pump–thaw cycles. C_6H_6 vapor was entrained by bubbling Ar carrier gas through liquid benzene at ambient pressure and 15.0 °C. The C_6H_6 bubbler consisted of a glass vacuum trap placed inside a water bath in a dewar vessel. The temperature of this bath was maintained by running tap water through a coiled copper tube immersed in the bath and surrounding the C_6H_6 bubbler; the temperature was stable to better than ±0.5 °C over the time of the experiments. This temperature variation corresponds to a ±2% uncertainty in the C_6H_6 vapor pressure. The vapor pressure of the C_6H_6 at 15 °C was measured separately with a Hg manometer and was found to agree with ref 20. During the experiments the C_6H_6 concentration in the carrier gas (downstream of the bubbler) was monitored continuously by UV absorption at 253.7 nm (Hg pen ray lamp). The absorption cross section measured at 25 °C in Ar diluent, 1 atm total pressure, was 3.58×10^{-19} cm^2, in good agreement with the value reported in ref 10. No significant changes in absorption were observed during the kinetic measurement at all C_6H_6/Ar flows used, indicating complete saturation of the Ar carrier gas.

Heated lines and valves prevented condensation of the H_2O and C_6H_6 vapors downstream of the bubblers. The H_2O/Ar and C_6H_6/Ar flows were metered with calibrated inverted burets. H_2O and C_6H_6 concentrations in the reactor were calculated from the saturation vapor pressure at the bubbler temperatures, the reaction zone temperature and pressure, and the measured flow rates. The combined uncertainties in C_6H_6 and H_2O vapor pressure in the bubblers, in the metering of gases, and in the measurement of reactor temperature and pressure resulted in an estimated total uncertainty of about 10% for the $[H_2O]$ and $[C_6H_6]$ in the HTP reaction zone.

The temperature in the reaction zone was measured before and after each set of experiments with a shielded thermocouple.[19] The reported value is the average of these two measurements. The uncertainty in these measurements was estimated[19] at ±1%, plus any drift observed over the time of the experiments.

The optical plane of the HTP reactor is shown in Figure 1. The OH radicals are produced by vacuum ultraviolet photodissociation of H_2O vapor using a flashlamp (0.5–2.0 atm of Ar, 30–90 J, self-triggered, ca. 1 flash/s). LiF ($\lambda > 105$ nm) or Suprasil ($\lambda > 160$ nm) windows were used between the lamp and the reactor.

(20) "CRC Handbook of Chemistry and Physics"; 63rd ed, Weast, R. C., Astle, M. J., Eds.; CRC Press: Boca Raton, 1982; p D-221.

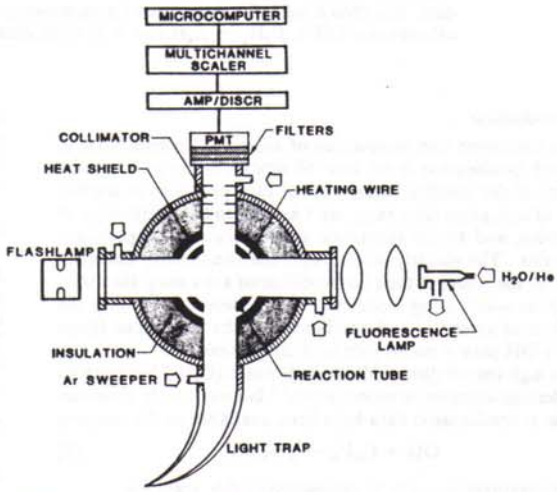

Figure 1. Optical plane of HTP reactor.

Flash pulse widths were less than 50 μs, i.e., much shorter than the chemical time scales of the OH/C_6H_6 studies. The initial rise in the output of a photodiode placed near the flashlamp was used to trigger the detection electronics (see below).

OH($A^2\Sigma \rightarrow X^2\Pi$) resonance radiation to monitor the relative OH concentration was provided by a microwave excited diagnostic flow lamp (3% H_2O in Ar, 4.0 kPa total pressure). The OH resonance radiation fluorescence was viewed at right angles to the flow and to the flash and diagnostic lamps through light collection optics and an interference filter (310 nm, 20% peak transmission, 10 nm bandwidth) by a cooled photomultiplier tube (EMI 9558QA). To eliminate PMT overload from scattered flashlamp radiation and from fluorescence by OH($A^2\Sigma^+$) produced during the flash, a variable delay gate was used to apply the cathode to first dynode voltage only during the period over which kinetic measurements were performed (typically 1–100 ms after the flash). This permitted measurements of first-order rate coefficients as high as ca. 1000 s^{-1}.

The time-dependent fluorescence intensity, $I(t)$, which is directly proportional to the OH concentration, $[OH]_t$, was measured by accumulating signal over 250–2000 flashes using a multichannel scaler (100 μs/channel); the accumulated signal was then transferred to a microcomputer for analysis.

III. Results

A. Kinetic Measurements. Measurements of the overall rate coefficient for the OH + C_6H_6 reaction were obtained over the temperature range 790–1410 K. At each temperature, the rate coefficients were determined by analyzing OH decay traces obtained at different C_6H_6 concentrations. The experimental conditions of the measurements are summarized in Table I. We have previously[18] estimated that initial OH concentrations, $[OH]_0$, produced in the HTP reactor by the flash photolysis (LiF optics)

of H_2O, are in the range (1–10) × 10^{10} molecules cm^{-3}. By comparison, it is seen in Table I that benzene concentrations, $[C_6H_6]$, ranged over (1.3–34) × 10^{13} molecules cm^{-3}, and are thus in excess by at least 100-fold. Under these conditions, only pseudo-first-order kinetics are expected to affect the temporal variation of the OH concentrations, with radical–radical reactions occurring at negligible rates. In the absence of complicating secondary reactions, the relaxation of $[OH]_t$ is then given by the expression

$$[OH]_t = [OH]_0 \exp[-(p_{OH} + k_1[C_6H_6])t] \quad (A)$$

where p_{OH} is the approximately first-order rate coefficient for the removal of OH from the viewing zone by flow and diffusion.

Fluorescence intensity profiles, $I(t) \propto [OH]_t$, obtained at temperatures below ca. 1000 K were observed to be accurately described by a single exponential decay, and were therefore fitted with the expression

$$I(t) = a_1 \exp(-a_2 t) \quad (B)$$

The kinetic information is contained in the parameter a_2, which by comparison with eq A is given as

$$a_2 = p_{OH} + k_1[C_6H_6] \quad (C)$$

At temperatures higher than about 1000 K, we have previously shown that the reaction

$$H + H_2O \rightarrow OH + H_2 \quad (2)$$

can be a significant secondary source of OH and can result in the appearance of maxima in $[OH]_t$ several milliseconds after the flash. The OH profiles are then properly described by the superposition of two exponential terms, one for the removal of OH, the other for the removal of H atoms. In the previous work,[17] this secondary OH generation was used to measure the rate coefficient k_2 for the H + H_2O reaction. For the purpose of the present study, it should be noted that H atoms diffuse out of the observation zone much more rapidly than OH radicals, so that the [OH] produced via reaction 2 is significantly smaller than the photolytically generated concentration, $[OH]_0$, which therefore accounts for most of the observed OH fluorescence signal. Removal of H atoms by C_6H_6 is, however, not believed to be rapid (based on an upper limit rate constant estimate of ref 21), so that a correction for the H + H_2O reaction was applied to the data obtained at $T > 1000$ K. The effect of this correction is rather small, yielding values of k_1 about 10–30% higher than those estimated with the single exponential decay approximation, eq A–C. The corrected and uncorrected values are shown in Table I.

The correction is based on the following kinetic scheme:

$$H_2O + h\nu \rightarrow OH + H$$

$$OH \rightarrow \text{first-order loss by flow and diffusion, } p_{OH},\ s^{-1}$$

$$H \rightarrow \text{first-order loss by flow and diffusion, } p_H,\ s^{-1}$$

$$OH + C_6H_6 \rightarrow \text{products} \qquad k_1(T)$$

$$H + H_2O \rightarrow OH + H_2 \qquad k_2(T)$$

Solution of the rate equation for $[OH]_t$ then gives

$$[OH]_t = a_1 e^{-(p_{OH}+a_2')t}\left\{1 + \frac{k_2[H_2O][1 - e^{-(p_H - p_{OH} + k_2[H_2O] - a_2')t}]}{p_H - p_{OH} + k_2[H_2O] - a_2'}\right\} \quad (D)$$

where $a_1 = [OH]_0$ and $a_2' = k_1[C_6H_6]$.

In eq D, all parameters except a_1 and a_2' can be estimated a priori. The value of k_2 is obtained from our recent direct measurement on this reaction.[17] In that work we also reported the value $(p_H - p_{OH}) \simeq 117\ s^{-1}$ at 26.7 kPa and 1274 K; since this term accounts for the difference in diffusion coefficients of OH and H in Ar, we have used this value, scaled to the present temperatures and pressures (P in kPa, T in K), with the expression

$$(p_H - p_{OH}) \simeq 117\ s^{-1}\ (26.7/P)(T/1274)^{3/2} \quad (E)$$

The $[C_6H_6]$ and $[H_2O]$ are, of course, measured directly, and p_{OH} was estimated from the uncorrected data. OH decay traces are then fitted with eq D to determine the two free parameters a_1 and a_2'.

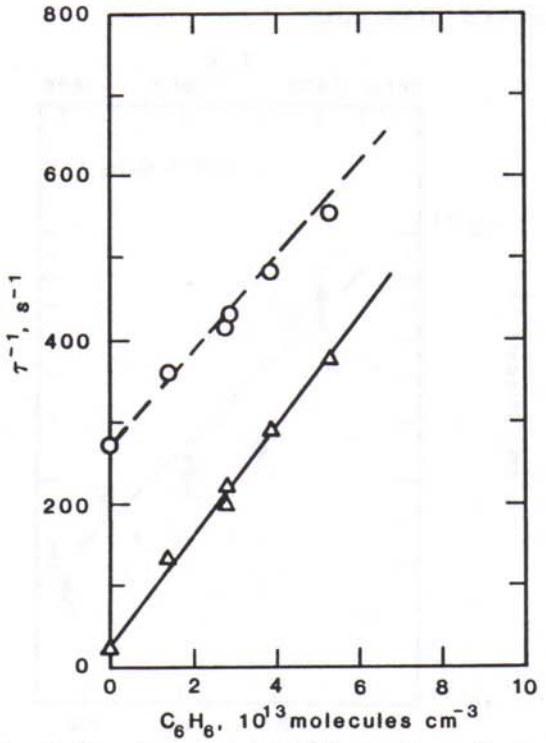

Figure 2. First-order decay rates at 1309 K: ○, a_2 from eq C, uncorrected for H + H_2O; △, a_2' from eq D, corrected for H + H_2O.

Values of the fitting parameters a_2 (from the uncorrected expression, eq C) and a_2' (from the corrected expression, eq E) were evaluated from the OH decay profiles using the weighted nonlinear least-squares fitting procedure described previously.[17,18] The results are shown in Figure 2 as a function of C_6H_6 for the measurements obtained at 1309 K. As predicted, the values of a_2' ($\simeq k_1[C_6H_6]$) display a nearly zero intercept, while the values of a_2 ($\simeq p_{OH} + k_1[C_6H_6]$) do not. The line defined by a_2' could be shifted vertically by using slightly different (e.g., 20% changes) choices of the fixed parameters p_{OH}, $p_H - p_{OH}$, or k_2, but the slope of the line ($= k_1$) was remarkably insensitive to these parameters. For the case illustrated in Figure 2, the correction predicts a k_1 value about 16% higher than that obtained from the uncorrected fit.

The OH/C_6H_6 rate coefficients measured over 790–1410 K are summarized in Arrhenius form in Figure 3. No systematic differences appear between data obtained with LiF and with Suprasil optics. A simple Arrhenius expression representing these data

$$k_1(T) = (3.5 \pm 0.3) \times 10^{-11} \exp[-(2300 \pm 100)/T]\ cm^3\ s^{-1} \quad (790–1410\ K) \quad (F)$$

was obtained by fitting ln k (T) vs. $1/T$ with a straight line using the LINFIT code given by Bevington,[23] with the statistical weight of each datum taken as $(k/\sigma_k)^2$ (cf. Table I for individual values). Inclusion of uncertainties due to temperature measurement (estimated as $\sigma_T\ \partial k/\partial T$) did not significantly alter the Arrhenius parameters and their uncertainties.

(21) Nicovich, J. M.; Ravishankara, A. R. *J. Phys. Chem.* **1984**, *88*, 2534.
(22) Bevington, P. R. "Data Reduction and Error Analysis for the Physical Sciences"; McGraw-Hill: New York, 1969.

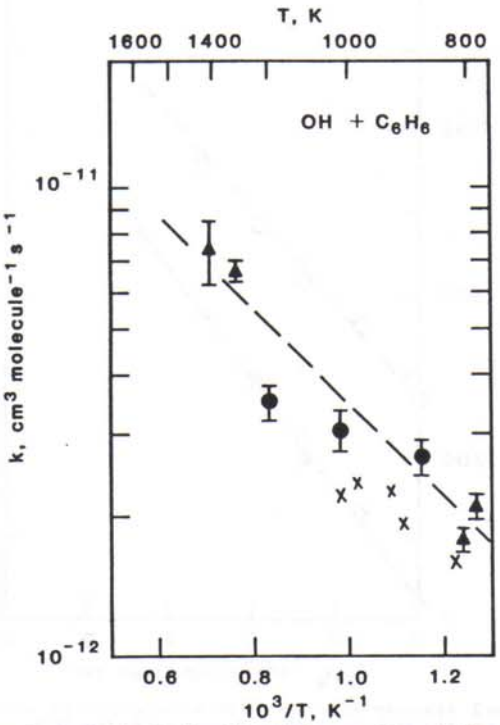

Figure 3. Arrhenius plot for OH + C_6H_6: ●, this work, Suprasil flashlamp optics; ▲, this work, LiF flashlamp optics; ×, from ref 10.

The activation energy measured for reaction 1 in the present work agrees well with the earlier, lower temperature results of Tully et al.,[10] but the preexponential factor found in that earlier work is some 30% lower than that obtained in the present study. The origin of this rather small discrepancy is not clear, but it may be related to systematic experimental errors in one of the studies (e.g., C_6H_6 metering), rather than to secondary kinetic effects. For example, it appears unlikely that the correction for the H + H_2O reaction is related to this discrepancy, since the present values exceed those of ref 10 in the temperature range at which the two studies overlap (790 to 1020 K, where the kinetic effect of the H + H_2O reaction is negligible), as well as at higher temperatures where the present, corrected values are still higher than the extrapolated expression of ref 10.

B. Mechanistic Studies (1314 K). The effects of the H + H_2O reaction (reaction 2) on OH temporal profiles, which were quantified in an earlier publication,[17] provide an opportunity to resolve existing questions on the identity of the products of the OH + C_6H_6 reaction. As outlined in section I, two different reaction channels have been proposed:

$$OH + C_6H_6 \rightarrow C_6H_5 + H_2O \quad (1a)$$

$$\rightleftarrows C_6H_6OH^{\dagger} \rightarrow C_6H_5OH + H \quad (1b)$$

In the context of the present work, we noted that, for both reactions 1a and 1b, one of the products may react with H_2O (present in large excess in our experiments, as the photolytic parent for OH) as follows:

$$C_6H_5 + H_2O \rightarrow OH + C_6H_6 \quad (-1a)$$

$$H + H_2O \rightarrow OH + H_2 \quad (2)$$

These reactions are qualitatively similar, because both regenerate OH (the species being monitored), but may differ quantitatively in their respective rate coefficient values. Since the rate coefficient for reaction 2 is known,[17] we hypothesized that it might be possible to discriminate between the channel producing C_6H_5 (abstraction) and that producing H atoms (H elimination), simply by measuring the extent to which secondary OH radicals are produced when the H_2O concentration is suitably increased.

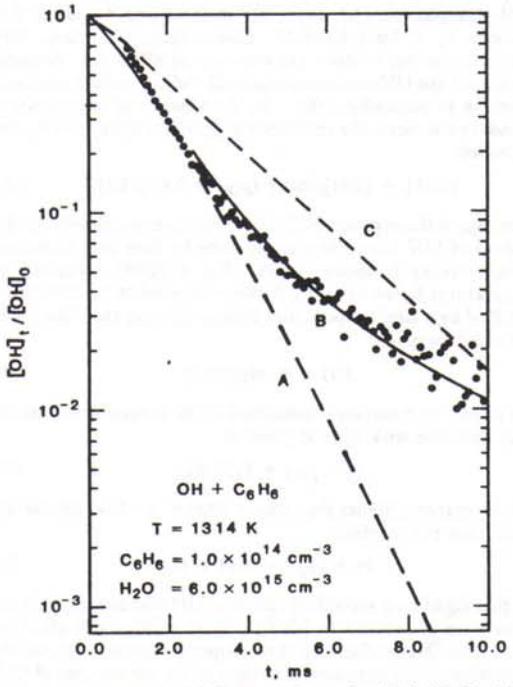

Figure 4. Nonexponential OH decay observed at high [H_2O]. The predictions of numerical simulation based on different OH + C_6H_6 reaction mechanisms are also shown: model A, abstraction only; model B, abstraction and reverse reaction; model C, H atom elimination. For details, see text.

TABLE II: Input Parameters for Numerical Simulation

		source
T, K	1314	*a*
P, kPa	11.7	*a*
[H_2O], cm^{-3}	6.00×10^{15}	*a*
[C_6H_6], cm^{-3}	1.0×10^{14}	*a*
k_1, $cm^3\ s^{-1}$	6.66×10^{-12}	*b*
k_2, $cm^3\ s^{-1}$	1.04×10^{-13}	*c*
k_{-1a}, $cm^3\ s^{-1}$	1.06×10^{-14}	*d*
p_{OH}, s^{-1}	290	*b*
p_H, s^{-1}	570	*e*
$p_{C_6H_5}$, s^{-1}	250	*e*

[a] From experimental conditions. [b] From kinetic measurements at low [H_2O]. [c] Reference 17. [d] Estimated from forward rate coefficients and thermochemical data.[23] [e] Estimated, see text.

Such measurements, designed to distinguish between these reaction channels, were performed at 1314 K, at the experimental conditions listed in Table I. A typical experimental [OH] temporal profile is shown in Figure 4. Qualitatively similar OH decay traces were obtained over the entire range of [C_6H_6] in these experiments. The strong curvature seen in Figure 4 was present only at high [H_2O]; at equal temperature (1310 K, cf. Table I), total pressure, and flow rate, but low [H_2O] (e.g., 1.37×10^{15} cm^{-3}), it was unequivocally absent.

To interpret these OH decay traces in terms of specific reaction channels, we calculated the time evolution of the $[OH]_t$ by numerically integrating the rate equations for OH, H, and C_6H_5, based on three different reaction schemes.

The input values of the numerical models, appropriate to the conditions of the experimental OH temporal profile of Figure 4, are given in Table II. C_6H_6 and H_2O concentrations, temperature, and pressure were obtained from the experimental measurements. The values of k_1 and p_{OH} were obtained from measurements at low [H_2O], $T = 1309$ K (see Table I and Figure 2); k_2 was taken

TABLE III: Model Kinetic Scheme

mechanism	kinetic model[a] A	B	C
$H_2O + h\nu \rightarrow OH + H$	$[OH]_0 = [H]_0$	$[OH]_0 = [H]_0$	$[OH]_0 = [H]_0$
$H + H_2O \rightarrow OH + H_2$	k_2	k_2	k_2
$OH \rightarrow$ loss by flow and diffusion	p_{OH}	p_{OH}	p_{OH}
$H \rightarrow$ loss by flow and diffusion	p_H	p_H	p_H
$C_6H_5 \rightarrow$ loss by flow and diffusion	0	$p_{C_6H_5}$	0
$OH + C_6H_6 \rightarrow C_6H_5 + H_2O$	k_1	k_1	0
$OH + C_6H_6 \rightleftarrows C_6H_6OH^* \rightarrow C_6H_5OH + H$	0	0	k_1
$C_6H_5 + H_2O \rightarrow OH + C_6H_6$	0	k_{-1a}	0

[a] Values of k_1, k_2, k_{-1a}, p_{OH}, p_H, and $p_{C_6H_5}$ as in Table II.

from the expression recommended in ref 17; the equilibrium constant for reactions 1a and −1a was estimated from thermochemical data,[23] and used to calculate k_{-1a} from the measured value of k_{1a}; p_H was estimated from p_{OH} via eq E; the first-order flow and diffusion loss of C_6H_5, $p_{C_6H_5}$, was estimated from the expression

$$p_{C_6H_5} = p_H - (p_H - p_{OH})[1 - (\mu_H/\mu_{C_6H_5})^{1/2}]/[1 - (\mu_H/\mu_{OH})^{1/2}] \quad \text{(G)}$$

where μ_i is the reduced molecular mass of the ith subscripted species, in Ar diluent.

The results of the numerical integration, based on three different model reaction schemes (see below), are shown in Figure 4. The calculations have been normalized to unity at $t = 0$. The experimental points have similarly been divided by their estimated initial value. Except for this normalization at $t = 0$, there are no additional adjustable parameters in any of the three models.

The similarities and differences among models are illustrated in Table III. All three models included equal initial photolytically produced concentration of H and OH; flow and diffusion losses for the free radicals, H, OH, and C_6H_5; and secondary production of OH via the $H + H_2O$ reaction. The models, however, differ in the identity and subsequent fate of the products of the $OH + C_6H_6$ reaction.

In model A, only the abstraction reaction was considered

$$OH + C_6H_6 \rightarrow C_6H_5 + H_2O \qquad \text{(1a)}$$

and was assigned a rate coefficient $k_{1a} = k_1$ (see Table II). The rate coefficients k_{-1a} (reverse reaction) and k_{1b} (H atom elimination) were set to zero. The calculation shows that the OH temporal decay over 0.0–1.0 ms is slightly slower than that at longer times, due to the conversion of photolytically generated H atoms, $[H]_0$, to OH via reaction 2. Beyond 1 ms, only reaction 1a and flow and diffusion loss of OH contribute to the OH profile. The experimental OH profile is seen to agree well with this model up to about 3 ms.

In model B, both abstraction and the reverse reaction were included

$$OH + C_6H_6 \rightleftarrows C_6H_5 + H_2O \qquad \text{(1a, −1a)}$$

with rate coefficients $k_{1a} = k_1$ and k_{-1a} given in Table II. The rate coefficient for H atom elimination, k_{1b}, was again set to zero. The conversion of $[H]_0$ to OH is again discernible at $t < 1$ ms, followed by a faster decay over 1–4 ms. At longer times, the regeneration of OH via reaction −1a is apparent. This model agrees with the experimental data at all times.

In model C, the rate coefficients for reactions 1a and −1a were set to zero, and the rate coefficient for the H atom elimination channel

$$OH + C_6H_6 \rightleftarrows C_6H_6OH^{\dagger} \rightarrow C_6H_5OH + H \qquad \text{(1b)}$$

was given the value (k_1) in Table II. The model shows that, if H atoms were produced in the $OH + C_6H_6$ reaction, reaction 2 would rapidly reconvert these to OH, resulting in OH decays which are considerably slower than those expected on the basis of the forward reaction rate coefficient k_{1b}. This model disagrees with the experimental data at all times.

Qualitatively similar results were obtained at different (cf. Table I) C_6H_6 concentrations. In all cases, the best agreement with experimental data was obtained with model B.

These results show that abstraction (reaction 1a) is the dominant reaction channel for $OH + C_6H_6$ near 1300 K. To estimate an upper limit on the contribution from channel 1b, numerical simulations were also carried out using the full reaction scheme shown in Table III with the values from Table II, assuming $k_1 = k_{1a} + k_{1b}$, and varying the branching ratio k_{1b}/k_1 from 0 to 1. The deviation of the calculated OH profiles from the data was smallest at $k_{1b}/k_1 = 0$ (as in model B above), and increased monotonically as the branching ratio was increased. At $k_{1b}/k_1 = 0.2$, the deviation is obviously so large that we conclude, quite conservatively, that the abstraction reaction accounts for at least 80% of the overall reaction rate coefficient:

$$k_{1a}/k_{1b} > 4$$

In separate numerical simulations, the value of the rate coefficient k_{-1a} for the $C_6H_5 + H_2O$ reaction was varied by ±30% from the thermochemically calculated value of Table II. These variations produced clear deviations between the model calculation (model B) and the experimental OH decay profiles, leading to the estimated experimental value

$$k_{-1a}(1314\ \text{K}) \simeq (1.0 \pm 0.3) \times 10^{-14}\ \text{cm}^3\ \text{s}^{-1}$$

To our knowledge, this is the first experimental determination of this rate coefficient by any method.

The mechanistic inferences made from the above study are based on two observations from data such as those shown in Figure 4: (1) the absence of secondary H atoms, under conditions where they should be detected via the $H + H_2O$ reaction, and (2) the regeneration of OH, by reaction of H_2O with another species, with a rate coefficient of $\approx 1 \times 10^{-14}$ cm^3 s^{-1}, i.e., in excellent agreement with the value predicted for reaction −1a if the forward channel is attributed to abstraction. Both observations independently support abstraction as the dominant $OH + C_6H_6$ channel. Alternative explanations, in which the H atom elimination channel 1b is dominant, do not seem plausible. Secondary reactions which do not involve C_6H_6 or H_2O as one of the reagents are unimportant because of the low concentrations of all other species. Another possibility which can account for the failure to observe secondary H atoms is that the hypothetical channel 1b is followed by the reaction

$$H + C_6H_6 \rightarrow C_6H_5 + H_2 \qquad \text{(3)}$$

For this reaction to compete with reaction 2 would require a rate coefficient $k_3 > 6 \times 10^{-12}$ cm^3 s^{-1} at the H_2O and C_6H_6 concentrations used in the present experiments (see Table II). This value of k_3 is some 30 times larger than the value calculated for 1300 K from the upper limit expression given by Nicovich and Ravishankara.[21] While this seems improbable, more accurate, direct measurements of k_3 at high temperatures are certainly desirable. However, even if reaction 3 were much more rapid than currently believed, it would be difficult to explain the observed slow regeneration of OH observed at long times (see Figure 4) by a mechanism other than the reversible reaction 1a + −1a, as

(23) Benson, S. W. "Thermochemical Kinetics"; Wiley: New York, 1976; 2nd ed.

proposed above. Indeed, all OH + C_6H_6 reaction channels which do not lead to OH regeneration (via secondary reaction with H_2O) would produce OH decay traces similar to that of model A in Figure 4, i.e., inconsistent with the observed experimental decays.

The photodissociation of C_6H_6 by the vacuum-UV actinic flash might also be thought to interfere, to the extent that it affects the assumption $[H]_0 = [OH]_0$ used in the models. We estimated the extent of C_6H_6 photodissociation by averaging absorption cross sections for H_2O ($\sim 5 \times 10^{-18}$ cm^2) and for C_6H_6 ($\sim 1 \times 10^{-16}$ cm^2) over the vacuum-UV actinic flux region and further assuming that the quantum yield of H from C_6H_6 photodissociation is unity. This results in $1.0 < [H]_0/[OH]_0 < 1.3$, for the H_2O and C_6H_6 concentrations given in Table II. Therefore, the assumption $[H]_0 \approx [OH]_0$ appears to be reasonable. More importantly, the model calculations are remarkably insensitive to the initial H atom concentration, in the time period which overlaps with experimental data. For example, even taking $[H]_0 = 10[OH]_0$, the profiles predicted by the three models in Figure 4 are affected only at early time (e.g., <1 ms), where the large $[H]_0$ is rapidly converted to [OH]. At longer times, OH profiles are similar in shape to that shown in Figure 4, but correspond to a higher effective value of $[OH]_0$. Specifically, the low slope predicted for model C and the curved profile of model B are still quantitatively predicted. The shapes of the experimental profiles, which are obtained only for times > ≈1 ms, agree only with model B even at these artificially high initial H atom concentrations. Inclusion of high initial concentrations of phenyl radicals, e.g., $[C_6H_5]_0 = [H]_0 - [OH]_0$ as might be expected from C_6H_6 photodissociation, leads to similar conclusions.

Acknowledgment. This work was supported by NASA-Lewis Research Center, Aeronautics Section, Cleveland, OH, under Contract No. NAS3-24345. We thank E. R. Lezberg (NASA-Lewis) for his support and J. H. Lee (Brookhaven National Laboratory) for helpful suggestions on OH lamp optics.

Registry No. OH, 3352-57-6; C_6H_6, 71-43-2.